GEOLOGY

Metamorphic diamond from the northeastern margin of Gondwana: Paradigm shifting implications for one of Earth's largest orogens

Alexander Edgar[1]*, Ioan V. Sanislav[1], Paul H. G. M. Dirks[1], Carl Spandler[2]

We describe the first occurrence of diamond-facies ultrahigh pressure metamorphism along the Gondwana-Pacific margin of the Terra Australis Orogen. Metamorphic garnet grains from Ordovician metasediments along the Clarke River Fault in northeastern Queensland contain inclusions of diamond and quartz after coesite, as well as exsolution lamellae of rutile, apatite, amphibole, and silica. These features constrain minimum pressure-temperature conditions to >3.5 gigapascals and ~860°C, although peak pressure conditions may have exceeded 5 gigapascals. On the basis of these data, we interpret the Clarke River Fault to represent a Paleozoic suture zone and at least parts of the Terra Australis Orogen to have formed through classic Wilson cycle processes. The growth of the Terra Australis Orogen during the Paleozoic is largely attributed to accretionary style tectonics. These previously unknown findings indicate that the Terra Australis Orogen was not just a simple accretionary style orogen but rather a complex system with multiple tectonic styles operating in tandem including collisional tectonics.

INTRODUCTION

Background

The identification of ultrahigh pressure (UHP) metamorphism is important for the tectonic reconstruction of ancient terranes. UHP metamorphism is typically interpreted to indicate collisional orogenesis and deep subduction (>70 km) of continental material (*1*–*4*). Continental material may be subducted to depths >200 km (*5*–*7*) before exhumation and emplacement along continental suture zones. Although UHP metamorphic rocks have been proposed to form in a range of geodynamic environments (*8*), to date, in situ UHP assemblages, particularly those recording extreme pressure conditions (>5 GPa), are constrained to collisional orogens.

Records of UHP metamorphism have been linked to mineralogy and mineral textures of metamorphic rocks (*9*). The existence of coesite and metamorphic diamond in continental rocks is widely regarded as robust evidence for UHP metamorphism (*6*, *10*, *11*). The mineralogy of exsolution phases in metamorphic garnet and pyroxene, including rutile, ilmenite, apatite, amphibole, clinopyroxene, and quartz, has also been used to constrain HP/UHP metamorphic conditions (*12*, *13*), with silicate exsolution in garnet considered evidence of former supersilicic, majoritic garnet and therefore extreme pressure conditions (*4*, *6*).

The Neoproterozoic-Paleozoic Terra Australis Orogen represents a long-lived accretionary margin that extended for >18,000 km along the paleo-Pacific margin of the Gondwana supercontinent (Fig. 1) (*14*). The Terra Australis Orogen is considered to be a type example of orogenesis without collision (*15*) and comprises the Tasmanides in Australia, the Ross Orogen in Antarctica, the Cape Basin of South Africa, and Neoproterozoic-Paleozoic orogens of the Andean Cordillera in South America. To date, there have been no reports of diamond-facies UHP metamorphism within the Terra Australis Orogen. Paleozoic tectonic models describing the Terra Australis Orogen in eastern Australia (i.e., northeastern margin of Gondwana) describe an accretionary environment with continent growth occurring via a westward-dipping, eastward-migrating subduction complex without the addition of exotic continental terranes (*16*–*18*). The northernmost portion of this accretionary margin, located in north Queensland, has seen comparatively little study.

Here, we present evidence for Wilson cycle–style tectonics within the Terra Australis Orogen, including ocean closure and continent collision. Diamond-facies UHP metamorphism is preserved in metamorphic garnets from quartzites within the Ordovician Running River Metamorphics of northeast Queensland. These garnets contain inclusions of metamorphic diamond and pseudomorphs of coesite and display exsolution lamellae of oxide and silicate minerals characteristic of continental crust subducted to >100 km depth. This is the first record of diamond-facies UHP metamorphism in Australia, and it provides crucial constraints for the tectonic processes operating throughout one of the largest orogens in Earth's history.

Geological setting

The geology of eastern Australia is dominated by the Neoproterozoic-Paleozoic rocks of the Tasmanides. The Tasmanides are a collage of five major orogens; the Delamarian, Lachlan, Thomson, Mossman, and New England Orogens. The Paleozoic rocks of the Tasmanides in northeast Queensland have been subdivided into the Thomson and Mossman Orogens (Fig. 1) (*16*, *19*, *20*). The northern extent of the Thomson Orogen is represented by the Cambro-Ordovician Charters Towers Province, which has been interpreted to consist of a sequence of metasedimentary and meta-igneous rocks formed in a continental back-arc setting (*21*). The southern extent of the Mossman Orogen, which is in fault contact with the Charters Towers Province along the Clarke River Fault, is represented by the Broken River Province. The Broken River Province consists of a series of marine metasediments and tectonic mélange interpreted to represent a forearc active margin assemblage (*18*, *19*, *22*). The Charters Towers and the Broken River Provinces are intruded by extensive suites of Permo-Carboniferous felsic plutons (*18*, *19*, *21*, *23*).

[1]College of Science and Engineering, Economic Geology Research Centre (EGRU), James Cook University, Townsville, Australia. [2]Department of Earth Sciences, The University of Adelaide, Adelaide, Australia.
*Corresponding author. Email: alexander.edgar@my.jcu.edu.au

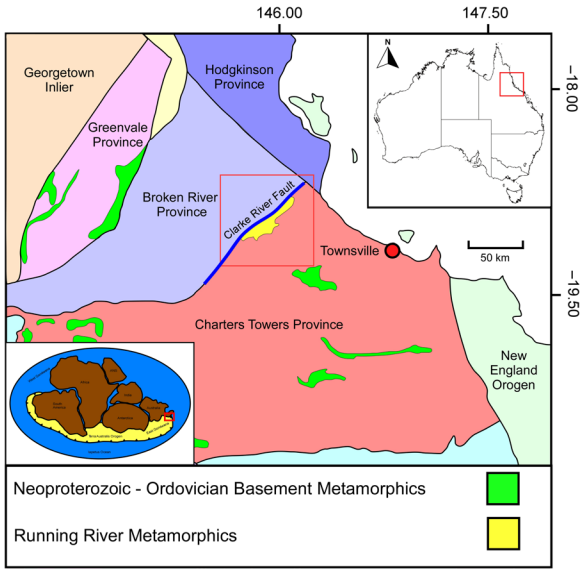

Fig. 1. Northeast Queensland tectonic framework. Tectonic framework for Northeast Queensland depicting major provinces of the northern Thompson Orogen and southern Mossman Orogen. Red box highlights the location of the Running River Metamorphics (study site) along the Clarke River Fault: a major tectonic structure dividing the Thompson and Mossman Orogens. The bottom left inset map depicts the arrangement of the Gondwana supercontinent during the Paleozoic, with the Terra Australis Orogen extending along the eastern, southern, and western continental margins. ANS, Arabian-Nubian Shield.

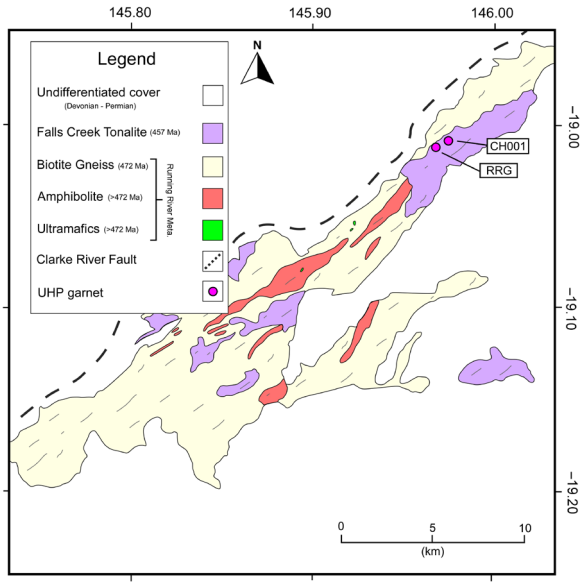

Fig. 2. Local geology. Local geology and sample sites of UHP garnet bearing quartzite for the Running River Metamorphics [modified from (*24*)]. The UHP garnet is sampled from meter-scale quartzite lenses, which occur as rafts along the Falls Creek Tonalite margins.

The Ordovician Running River Metamorphics (Fig. 2) are a suite of strongly deformed, amphibolite-facies basement rocks, belonging to the Charters Towers Province and positioned along the Clarke River Fault (*17*, *24*). They comprise amphibolite, felsic gneiss, quartzite, migmatite, rare lenses of ultramafic rocks, and the intrusive Falls Creek Tonalite. Dirks *et al.* (*24*) interpreted the amphibolite as obducted basaltic material, initially formed within an intra-oceanic plate setting, and the ultramafic rocks as lenses of ophiolitic material emplaced during accretion. The amphibolites are faulted against basement felsic gneiss (formerly S-type granite) (*24*). Lenses of quartzite, which commonly outcrop as rafts along intrusive margins, have maximum depositional ages of ~472 million years old (Ma) (*24*) and are spatially associated with the allochthonous blocks of amphibolite. The whole sequence has been intruded by the post-metamorphic, 456-Ma Falls Creek Tonalite (*24*). These relationships constrain the timing of metamorphism to between 456 and ~472 Ma.

Lithologies of the Running River Metamorphics

Felsic gneiss is the dominant rock type of the Running River Metamorphics. The gneiss has a well-developed gneissic foliation and consists of biotite, muscovite, quartz, and feldspar with minor amounts of garnet and cordierite. On the basis of the compositional homogeneity and the S-type geochemical affinity, the protolith of the felsic gneiss is interpreted to be a crustally derived granitic intrusion (*24*).

Amphibolite occurs as massive or laminated, northeast oriented, lenticular bodies, which were faulted against the felsic gneiss (*24*). It comprises mostly hornblende, plagioclase, clinopyroxene, and epidote, with accessory titanite. The amphibolite hosts a migmatitic leucosome phase of tonalitic composition that consists of plagioclase, quartz, hornblende, and minor clinopyroxene. The leucosomes are undeformed and are commonly observed to be along foliation planes and fractures within the amphibolite (*24*). The leucosome is interpreted to be the product of decompression melting during exhumation of the Running River Metamorphics. The amphibolite also contains numerous, tens of meter-scale occurrences of lenses of mafic-ultramafic rocks, including anthophyllite schist, hornblendite, and pyroxenite. To date, no relict evidence of UHP metamorphism has been identified with the amphibolite unit.

The quartzite occurs as meter-scale rafts within the Falls Creek Tonalite and is usually intercalated with amphibolite, suggesting a common origin. It consists mainly of quartz, with thin laminae rich in biotite, amphibole, garnet, and chlorite. The main accessory minerals are rutile, apatite, and zircon. Locally, a garnet-rich variety occurs and consists of alternating garnet- and quartz-rich domains. The garnet-rich domains consist mainly of garnet with retrograde chlorite and epidote, whereas the quartz-rich domains also contain phengite and apatite. In general, the garnet grains are intensely fractured and vary in size from <1 up to 5 mm. Some garnet grains have been boudinaged during deformation, and larger grains commonly display undulose extinction in crossed polarized light. The garnet grains are interpreted to be metamorphic in origin (as opposed to detrital) as most garnet grains are much coarser than the surrounding matrix, contain inclusions of the matrix minerals, and consist of multiple growth domains. Petrographic investigation and x-ray compositional mapping show the garnet grains to be concentrically zoned, consisting of core, mantle, and rim zones with distinct compositions, textures, and exsolution mineralogy. The garnet is spessartine-almandine rich and, from core to rim, displays decreasing Mn, Ca, and Ti content and increasing Fe and Mg content (fig. S3). The overall Mn-rich nature of the garnets is comparable to garnets from HP/UHP Mn-rich metasedimentary rock of ocean floor origin from the Western Alps (*25*). Garnet grains contain inclusions of

quartz, rutile, apatite, amphibole, carbonate, graphite, and diamond, as described in detail in the following section.

The Falls Creek Tonalite intrudes the felsic gneiss, amphibolite, and quartzite and occurs as a series of approximately northeast-southwest–oriented intrusive bodies. It has a well-developed foliation and consists of coarse-grained quartz and feldspar, with minor biotite, hornblende, and K-feldspar. The composition varies from tonalite to granodiorite (*24*).

RESULTS

Evidence for UHP metamorphism

The garnet cores and mantles commonly contain diamond inclusions (Fig. 3, A to C) and rutile (Fig. 3D), apatite (Fig. 3E), and amphibole (Fig. 3F) exsolution lamellae.

Metamorphic diamond

The garnet cores (Fig. 4A) contain 1- to 3-μm grains of metamorphic microdiamond that commonly occur within graphite, carbonate, or CO_2-rich fluid inclusions (Fig. 3, A to C). Thin sections were prepared without the use of diamond abrasives to eliminate the possibility of diamond contamination during sample preparation (Supplementary Materials). Raman spectra indicate a variable diamond peak with wave numbers in the range of 1319 to 1336 cm^{-1}, typically coexisting with a graphite peak (wave numbers range of 1570 to 1585 cm^{-1}) and carbonate or CO_2 fluid peak (wave numbers range of 1075 to 1085 cm^{-1}). The larger diamond grains have a very sharp diamond peak (Fig. 3A) with only a minor graphite peak, whereas smaller diamond grains display a less pronounced diamond peak and a well-developed graphite peak (Fig. 3C). Many of the graphite grains display cubic crystallography suggestive of an earlier cubic carbon form before graphitization (*7*, *10*). The carbonate inclusions consist predominantly of calcite, but they display variable Raman peaks with wave numbers ranging from 1070 to 1095 cm^{-1}, possibly indicating various carbonate species. Diamond stability in continental rocks indicates pressures >3 to 4 GPa at ~600° to 900°C (*26*).

Coesite pseudomorphs

In some places, garnet core and mantle zones exhibit radial fracture patterns around quartz inclusions (Fig. 4B), which is a diagnostic feature formed in response to volume changes associated with the phase transition from coesite to quartz upon decompression (*6*, *27*–*29*). All of the coesite has retrogressed to quartz, and the radial fractures,

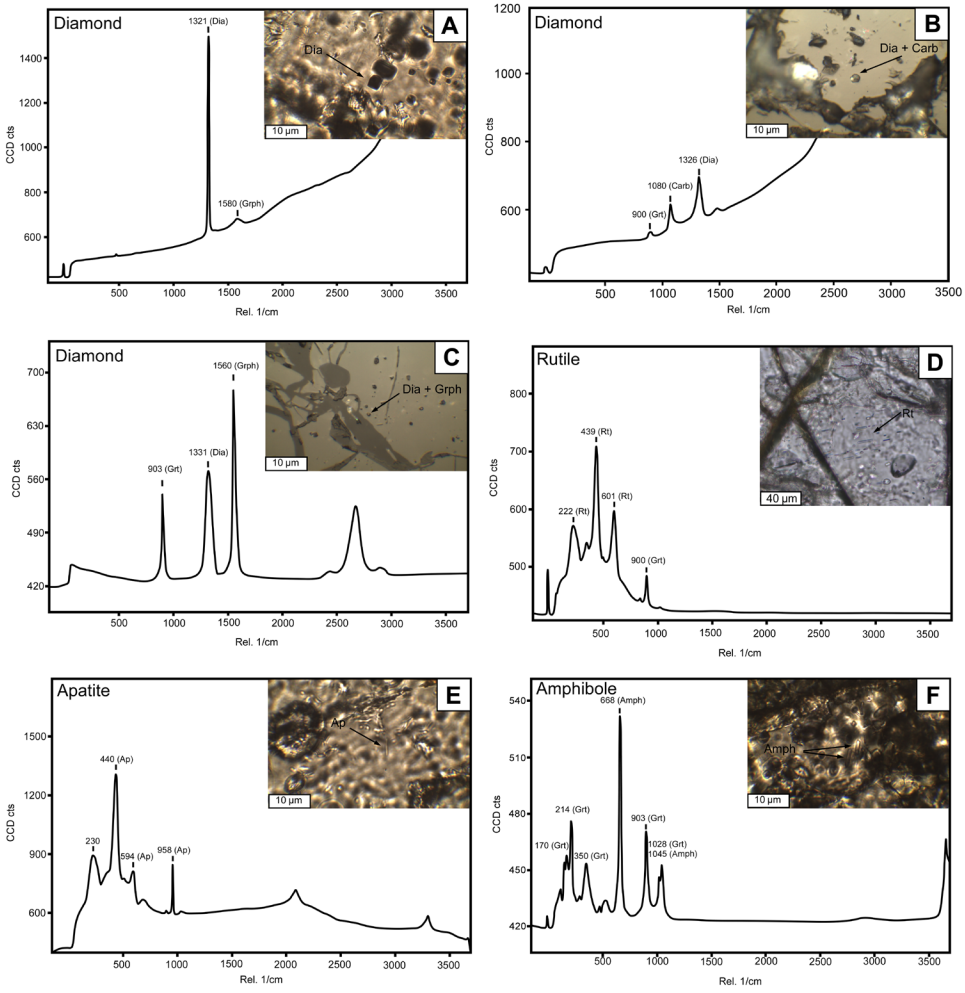

Fig. 3. Raman spectroscopy. Raman (532 nm) spectra of diagnostic HP/UHP garnet inclusions and exsolved minerals. CCD cts, charge couple device counts. Dia, diamond; Grph, graphite; Carb, carbonate; Rt, rutile; Grt, garnet; Ap, apatite; Amph, amphibole.

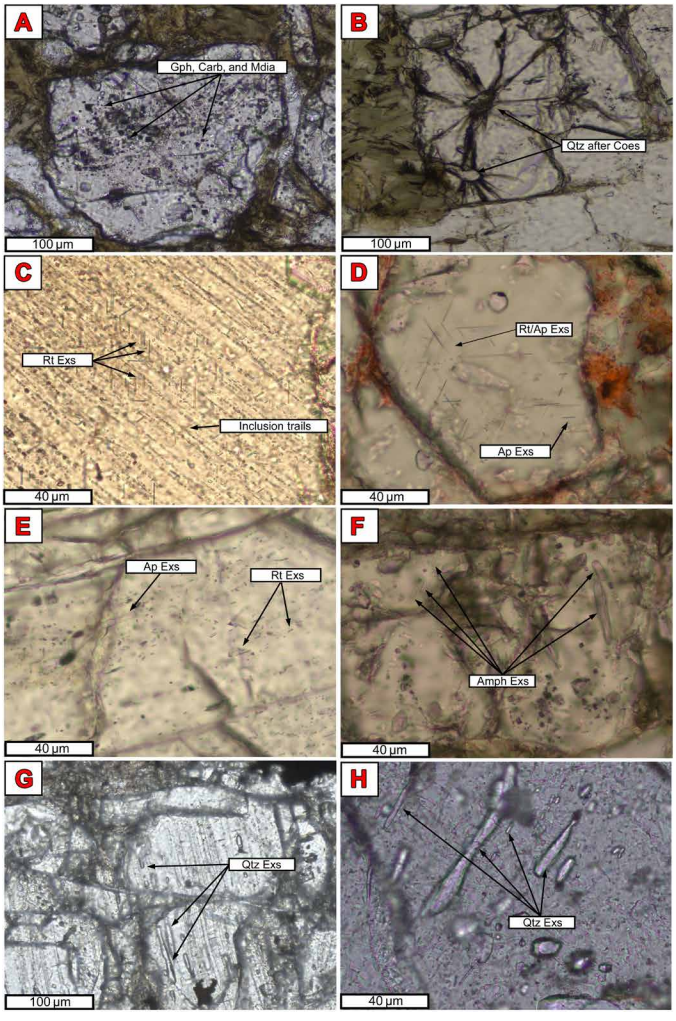

Fig. 4. Petrographic evidence. Evidence for UHP metamorphism: garnet inclusions and exsolution mineralogy. (**A**) Numerous orthogonal inclusions comprising carbonates (calcite, aragonite, dolomite, and Mg calcite), graphite, and microdiamonds. (**B**) Radial decompression fractures surrounding quartz interpreted to have formed after coesite. Fractures infilled by later chlorite. (**C**) Oriented inclusion trails and crystallographically controlled exsolution of rutile. (**D**) Numerous rutile and apatite exsolution needles. (**E**) Apatite and rutile exsolution lamellae. (**F**) Amphibole exsolution lamellae. (**G** and **H**) Quartz exsolution laths. Qtz, quartz; Coes, coesite; Mdia, microdiamond.

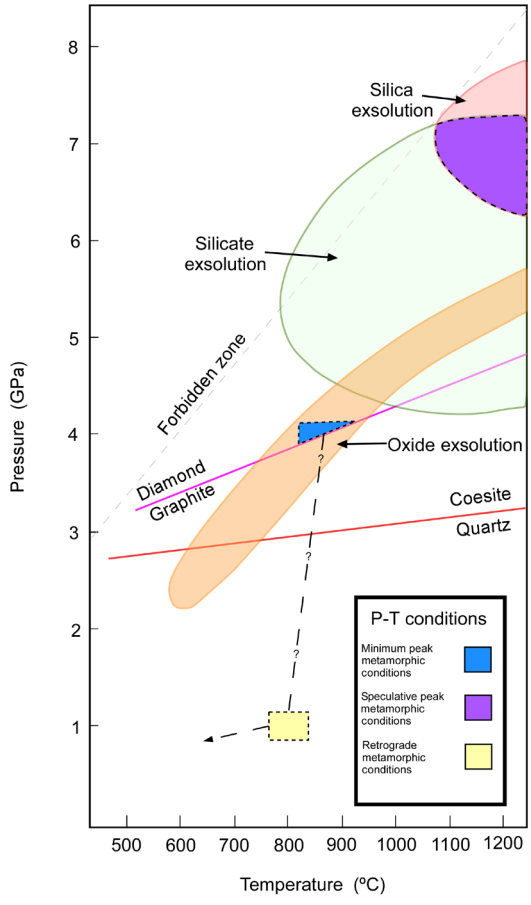

Fig. 5. P-T evolution. Proposed pressure-temperature (PT) conditions of the UHP garnet from the Running River Metamorphics. Exsolution mineralogy fields from (*4*). Minimum peak P-T conditions (blue triangle) of 3.5 to 4 GPa at 800° to 900°C are constrained by metamorphic diamond inclusions and Zr in rutile thermometry. Speculative peak P-T conditions (purple zone) are suggested by potential silicate and silica exsolution. Retrograde metamorphic conditions (yellow box) of 0.9 to 1.3 GPa at 750° to 850°C are constrained by Zr in rutile thermometry and garnet-biotite thermobarometry.

which propagated outward to the garnet margins, have been infilled by later chlorite and mica. Evidence of former coesite is widely considered to constrain minimum conditions to ~2.7 GPa at ~600°C (Fig. 5) (*3*, *30*, *31*) and defines the transition to UHP metamorphism.

Rutile and apatite exsolution

Garnet cores contain needle-like rutile and apatite interpreted to have formed as a result of exsolution (Fig. 4, C to E). The needles show crystallographically preferred orientations and are typically interpreted to represent evidence of former Ti- and P-rich garnets grown under HP (*32*–*35*) and/or high-temperature (HT) conditions (*36*, *37*). Rutile exsolution in garnet has been described at pressure-temperature (P-T) conditions of >1 GPa and >600°C, while apatite exsolution is generally indicative of >3 GPa and >800°C (*4*).

Amphibole exsolution and supersilicic garnet

Several garnets display patchy zones of anisotropy associated with exsolution lamellae of amphibole (Fig. 4F). The lamellae appear crystallographically oriented, but the relationship of exsolution to garnet anisotropy is unclear. Amphibole exsolution in garnet may indicate former majoritic, supersilicic garnet (*4*) whereby excess Si was incorporated in place of Al in the octahedral site. Garnet cores host-oriented quartz laths, redolent of exsolution (Fig. 4, G and H). Silica exsolution lamellae oriented along crystallographic planes have been described from only three localities globally: the Greek Rhodope collisional margin (*6*); the kimberlite xenoliths in Yukutia (*38*); and the Appalachian Orogen collisional margin (*4*). They have been interpreted to indicate former majoritic garnet stable at extreme pressures > 5 GPa (*4*, *39*).

Metamorphic temperature constraints

With a mineral assemblage including quartz, zircon, and rutile, metamorphic temperatures for the quartzite can be determined using the Zr-in-rutile thermometer (*40*, *41*). Rutile inclusions hosted in garnet mantle zones yield Zr concentrations of 932 to 1025 parts

per million (ppm), while rutile grains hosted within garnet rims have 415 to 510 ppm Zr. Applying these Zr contents to the pressure-dependent, coesite-stable thermometer of Kohn (*41*) at 3.5 GPa gives average temperatures of 865°C for the garnet mantle and 776°C for the garnet rim. Similar temperatures of 862°C for the garnet mantle and 783°C for the garnet rim were determined using the pressure-dependent calibration of Tomkins *et al.* (*40*) and assuming a pressure of 3.5 GPa.

Garnet-biotite thermobarometry (*42*, *43*) of garnet rim compositions and biotite in contact with the garnet rim suggests retrograde P-T conditions of ~800°C and 1.1 GPa. This temperature estimate is consistent with the results of Zr-in-rutile thermometry from the garnet rims and is interpreted to indicate the matrix equilibration conditions. The quartzite preserves no evidence of retrograde high temperature overprints such as melting. This is consistent with a lack of metamorphic rim overgrowth on the detrital zircon grains from the quartzite (*24*). Garnet grains preserve major element growth zonation (fig. S3), which indicates that it is unlikely that these rocks experienced temperatures > 800°C for extended periods of time during peak or retrograde metamorphism, as the garnet major element composition would be expected to diffusively re-equilibrate at these temperatures (*44*). Alternatively, the dry nature of the host quartzite inhibited reequilibration during high temperature metamorphism.

DISCUSSION

UHP metamorphism along the northeastern Gondwana margin

On the basis of the presence of microdiamond inclusions in garnet and Zr-in-rutile thermometry, we estimate that the P-T conditions (Fig. 5) for the Running River Metamorphics involved diamond formation at UHP conditions of ~3.5 GPa and ~860°C. This discovery of in situ diamond represents the second indication of UHP metamorphism within the Tasmanides [after (*45*)] and the first report of diamond-facies metamorphism in Australia. Subsequent to UHP metamorphism, the Running River Metamorphics underwent isothermal decompression to ~1.1 GPa (from garnet-biotite thermometry) followed by cooling during exhumation (Fig. 5).

While the existence of numerous microdiamond inclusions in garnet core and mantle zones is considered unequivocal evidence for UHP metamorphism, there are also other textural features that are consistent with UHP conditions for the Running River quartzites. Exsolution of rutile and apatite in garnet may form over a range of P-T conditions of >1 GPa and >600°C and have commonly been observed in HP/UHP rocks. Radial fractures around quartz grains included in garnets are generally regarded as evidence of former coesite (and hence, UHP conditions) (*46*), although no coesite has been identified from the Running River Metamorphics to date, so this interpretation remains speculative.

Amphibole and silica exsolution lamellae in UHP terranes globally are rare but, when described, are attributed to extreme pressure conditions of >5 GPa (*4*). Therefore, the presence of amphibole and silica exsolution in garnet cores at Running River allows speculation that peak metamorphic conditions may have reached >5 GPa and up to 1200°C (Fig. 5). However, such extreme conditions would require extremely rapid subduction and subsequent exhumation cooling to preserve the observed major element zoning in garnet. Moreover, the amphibole and silica lamellae in garnets from the Running River Metamorphics, although texturally suggestive, cannot be attributed to exsolution with certainty. Further work will be required to test the validity of this hypothesis.

Wilson cycle style tectonics in the Terra Australis Orogen

The Terra Australis Orogen extended along the Gondwana margin of the paleo-Pacific Ocean and was interpreted as a typical accretionary orogen that did not form through the classic Wilson cycle (*14*, *15*). The traditional model involves a single, long-lived, westward-dipping subduction system, whereby crustal growth is attributed to the subduction of oceanic crust, an eastward-migrating margin, sediment accretion, and accordion-style tectonics (*21*, *47*–*50*). An alternative model (*51*), referred to as quantum tectonics, proposes that the remnant arc terrains (e.g., Macquarie arc and Gamilaroi arc) represent allochthonous island arcs accreted to the eastern margin of Australia. UHP metamorphism to ~2.7 GPa has been described from the southern New England Orogen (*45*). Because of significant age discrepancies of ~200 Ma between lenses of UHP rocks and their host country rocks, it was suggested that these UHP rocks were formed and stored within a subduction zone during >1000 km of eastward migration before they were exhumed and incorporated into the Devonian-Carboniferous forearc complex along the East Gondwana margin (*45*). This model implies that a single subduction complex was active throughout the 200-Ma period of initial burial, UHP metamorphism, and later exhumation and emplacement. However, the discovery of Ordovician UHP metamorphism associated with ophiolitic rock from the Running River Metamorphics may provide the first direct evidence involving ocean closure and continent collision (Fig. 6) and requires a reassessment of existing tectonic models for the Terra Australis Orogen and the eastern margin of Gondwana.

Diamond-facies UHP metamorphism is typically attributed to active subduction complexes and arc-continent or continent-continent collision (*1*, *2*, *52*, *53*). The Ordovician Running River Metamorphics have been interpreted as a tectonic sequence of obducted oceanic crust (amphibolite and oceanic metasediments) faulted against basement S-type granites (felsic gneiss) (*24*). The quartzite, due to its close association with the amphibolite and the lack of any other clastic sediments, was interpreted to represent metamorphosed pelagic sediments (Fig. 6) (*24*), a premise supported by the Mn-rich composition of garnets from the quartzite, as is characteristic of other examples of subducted oceanic sediments metamorphosed to UHP (*25*, *54*). UHP metamorphism within Mn-rich garnet grains further strengthens the interpretation that the amphibolite and the quartzite represented remnant oceanic crust (*24*) and suggests active subduction and obduction of oceanic crust along the Clarke River Fault at ~472 Ma (Fig. 6). The peak P-T conditions of the Running River Metamorphics are also consistent with modern geothermal conditions of oceanic crust subduction (*55*), supporting a similar cool thermal regime for subduction across the Phanerozoic (*56*).

Ocean closure facilitated by the subduction of oceanic crust along the Clarke River Fault at ~472 Ma (Fig. 6) has broad implications for Paleozoic tectonic models describing the evolution of the Terra Australis Orogen. The combination of UHP metamorphism to diamond facies associated with subduction and emplacement of oceanic crust, together with the tectonic position of the Running River Metamorphics along a major structure, suggests that the Clarke River Fault represents a Paleozoic suture zone between the

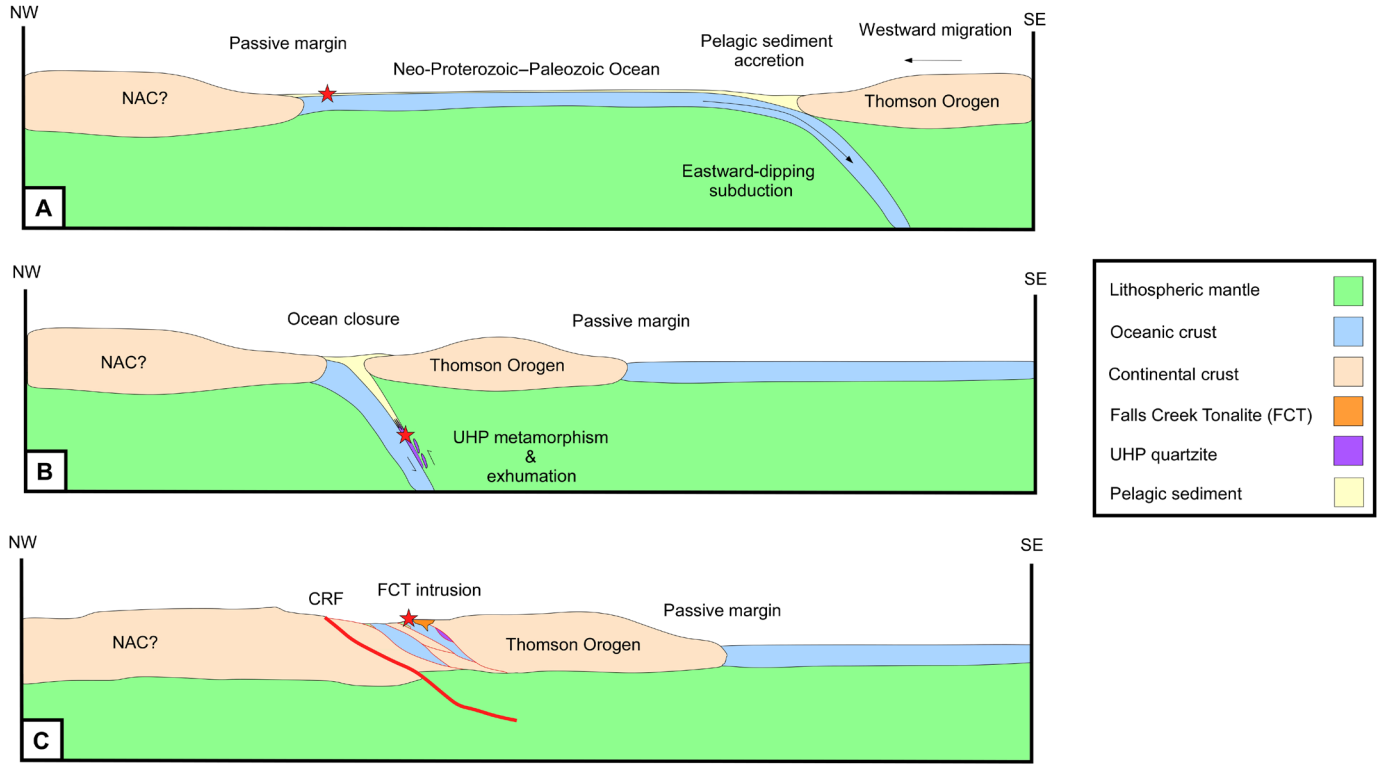

Fig. 6. Tectonic evolution. Proposed model depicting the tectonic evolution of the Running River Metamorphics. The red star icon tracks the evolution of quartzite. (**A**) The Thomson Orogen is positioned offboard of the North Australian Craton (NAC), separated by a Neo-Proterozoic–Paleozoic Ocean. The Thomson Orogen migrates westward, facilitated by an eastward-dipping subduction complex. The subduction of oceanic crust and westward migration of the Thomson Orogen results in the buildup of accreted pelagic sediment. (**B**) Continuous subduction of oceanic crust and the westward migration of the Thomson Orogen result in closure of the Neo-Proterozoic–Paleozoic Ocean. The accreted pelagic sediments are deeply subducted and metamorphosed under UHP conditions. Continuous subduction and eventual slab detachment result in exhumation of the UHP quartzite and amphibolite. (**C**) The UHP rocks are exhumed and tectonically juxtaposed against basement felsic gneiss sequences during continent suturing of the Thomson Orogen and the NAC along the Clarke River Fault (CRF). The exhumed metamorphic sequences are intruded and rafted by the Falls Creek Tonalite (FCT). NW, northwest; SE, southeast.

continental crust of the Thomson Orogen to the south and continental crust of unknown affinity to the north (Fig. 6). The Broken River Province, situated north of the Clarke River Fault, was interpreted to represent a Cambro-Devonian, westward-dipping subduction complex (*23*). Temporal overlap between an active, westward-dipping subduction complex within the Broken River Province and an active subduction complex along the Clarke River Fault suggests that multiple subduction complexes were active at ~472 Ma. In this case, the single, long-lived subduction model applied to the broader Tasmanides was not operational in northern Australia at least during the earliest Paleozoic. Subduction polarity along the Clarke River Fault is speculative, but the 456-Ma Falls Creek Tonalite, which intrudes the Running River Metamorphics, has been interpreted to have a continental magmatic arc affinity and may represent the product of continental arc magmatism above an easterly dipping subduction zone (Fig. 6). This would indicate that ocean closure was likely facilitated by either an eastward-dipping subduction complex (*51*) or an outward-dipping doubly subducting oceanic slab (*57*). Closure of oceanic crust and continent suturing along the Clarke River Fault (Fig. 6) indicates that at least parts of the Terra Australis Orogen experienced Wilson cycle–style tectonics. This implies that the Terra Australis Orogen was not a simple, continuous accretionary orogen but a complex margin with simultaneous contrasting tectonic styles and processes.

METHODS

Samples and petrography

UHP quartzite samples were collected from creek bed outcrops at Running River. The quartzite samples were collected from meter-scale quartzite rafts contained within the Falls Creek Tonalite. Two types of garnet are observed within the quartzite: coarse-grained flattened garnets sitting in biotite/amphibole-rich shear zones and fine-grained garnets in garnetite bands. UHP exsolution and inclusion minerals are observed in both the coarse-grained garnets and garnetite bands but are best preserved in the larger, shear zone garnets.

Polished thin sections of quartzite samples were prepared initially at Ingham Petrographics, Queensland, Australia. Following the discovery of diamond, a new set of thin sections were prepared by Adelaide Petrographics, South Australia, to eliminate the possibility of diamond contamination during thin section preparation. Rock slabs were initially cut and ground using a diamond saw and a fixed media diamond wheel. The rock slabs were then polished without the use of diamond abrasives in the final flattening of the sample (last 50 to 100 μm). The abrasive used to thin the rock slabs and to polish the thin sections consisted of very fine Si carbide paper, up to 7000 grit, as well as Al oxide and Ce oxide, and new polishing laps that had never been used before. The step-by-step procedure, provided by Adelaide Petrographics, is documented in the Supplementary

Methods. Subsequent analysis of the thin sections prepared at Adelaide Petrographics confirmed the presence of diamond in these samples, which we interpret to be of metamorphic origin.

Raman spectroscopy

Raman spectra were collected using the Witec UHTS 300 SMFC VIS-NIR Raman microscope with a 532-nm wavelength laser, housed within the Advanced Analytical Centre at James Cook University, Townsville. Data acquisition spanned 3 s, each with 10 acquisitions per measurement (30 s in total per measurement). Witec Control Four v4.1 software was used for all aspects of microscope control and data collection. The Raman microscope was regularly calibrated against crystalline silicon. Raman spectra of diamond were post-processed using the PeakFit software to better delineate peaks and define peak amplitudes and full widths at half maximum. Only diamond grains that occurred within the top 10 to 20 μm of the sample were targeted for analysis to avoid any potential contamination from the base of the slide.

Thermobarometric methods

Garnet-biotite thermobarometry was applied to establish P-T conditions during retrograde metamorphism. Garnet and biotite major element chemistry spot analyses were collected using a JEOL JXA 8200 electron probe microanalyzer (EPMA) housed at the Advanced Analytical Centre, James Cook University, Townsville. Measurement conditions included a 15-kV acceleration voltage, a 20-nA probe current, and a 5-μm probe diameter. Calibration standards are presented in table S1. Garnet major element maps were acquired using the same instrumentation and processed using ImageJ software to better establish chemical zonation patterns. Garnet and biotite major element data used for thermobarometry calculations are presented in tables S3 to S10. The data are presented in weight % oxide and atoms per formula unit.

The same electron microprobe facility was used in the analysis of Zr in rutile from garnet mantle and rim zones. This technique was applied to constrain metamorphic temperatures during garnet mantle and rim growth. Measurement conditions included a 20-kV acceleration voltage, a 100-nA probe current, and a 1-μm probe diameter. Experiment standards are presented in table S2. Rutile major element data used for thermobarometry calculations are presented in tables S11 and S12. The data are presented in weight % oxide, and Zr concentrations are given in parts per million.

SUPPLEMENTARY MATERIALS

Supplementary material for this article is available at https://science.org/doi/10.1126/sciadv.abo2811

REFERENCES AND NOTES

1. J. G. Liou, T. Tsujimori, R. Y. Zhang, I. Katayama, S. Maruyama, Global UHP metamorphism and continental subduction/collision: The Himalayan model. *Int. Geol. Rev.* **46**, 1–27 (2004).
2. M. Brown, Metamorphic conditions in orogenic belts: A record of secular change. *Int. Geol. Rev.* **49**, 193–234 (2007).
3. J. G. Liou, W. G. Ernst, R. Y. Zhang, T. Tsujimori, B. M. Jahn, Ultrahigh-pressure minerals and metamorphic terranes – The view from China. *J. Asian Earth Sci.* **35**, 199–231 (2009).
4. D. S. Keller, J. J. Ague, Quartz, mica, and amphibole exsolution from majoritic garnet reveals ultra-deep sediment subduction, Appalachian orogen. *Sci. Adv.* **6**, eaay5178 (2020).
5. K. Yi, B. Cong, D. Ye, The possible subduction of continental material to depths greater than 200 km. *Nature* **407**, 734–736 (2000).
6. E. D. Mposkos, D. K. Kostopoulos, Diamond, former coesite and supersilicic garnet in metasedimentary rocks from the Greek Rhodope: A new ultrahigh-pressure metamorphic province established. *Earth Planet. Sci. Lett.* **192**, 497–506 (2001).
7. W. E. Glassley, J. A. Korstgard, K. Sorensen, S. W. Platou, A new UHP metamorphic complex in the ~1.8 Ga Nagssugtoqidian Orogen of West Greenland. *Am. Mineral.* **99**, 1315–1334 (2014).
8. B. R. Hacker, T. V. Gerya, Paradigms, new and old, for ultrahigh-pressure tectonism. *Tectonophysics* **603**, 79–88 (2013).
9. J. A. Gilotti, The realm of ultrahigh-pressure metamorphism. *Elements* **9**, 255–260 (2013).
10. C. Chopin, Ultrahigh-pressure metamorphism: Tracing continental crust into the mantle. *Earth Planet. Sci. Lett.* **212**, 1–14 (2003).
11. L. F. Dobrzhinetskaya, Microdiamonds — Frontier of ultrahigh-pressure metamorphism: A review. *Gondw. Res.* **21**, 207–223 (2012).
12. I. Katayama, C. D. Parkinson, K. Okamoto, Y. Nakajima, S. Maruyama, Supersilicic clinopyroxene and silica exsolution in UHPM eclogite and pelitic gneiss from the Kokchetav massif, Kazakhstan. *Am. Mineral.* **85**, 1368–1374 (2000).
13. L. Liu, J. X. Yang, J. F. Zhang, D. L. Chen, C. Wang, W. Q. Yang, Exsolution microstructures in ultrahigh-pressure rocks: Progress, controversies and challenges. *Chin. Sci. Bull.* **54**, 1983–1995 (2009).
14. P. A. Cawood, Terra Australis Orogen: Rodinia breakup and development of the Pacific and Iapetus margins of Gondwana during the Neoproterozoic and Paleozoic. *Earth Sci. Rev.* **69**, 249–279 (2005).
15. P. A. Cawood, A. Kröner, W. J. Collins, T. M. Kusky, W. D. Mooney, B. F. Windley, Accretionary orogens through Earth history. *Geol. Soc. Lond. Spec. Publ.* **318**, 1–36 (2009).
16. R. A. Glen, The Tasmanides of eastern Australia. *Geol. Soc. Lond. Spec. Publ.* **246**, 23–96 (2005).
17. C. L. Fergusson, R. A. Henderson, I. W. Withnall, C. M. Fanning, D. Phillips, K. J. Lewthwaite, Structural, metamorphic, and geochronological constraints on alternating compression and extension in the Early Paleozoic Gondwanan Pacific margin, northeastern Australia. *Tectonics* **26**, TC3008 (2007).
18. I. W. Withnall, R. A. Henderson, Accretion on the long-lived continental margin of northeastern Australia. *Episodes* **35**, 166–176 (2012).
19. I. W. Withnall, L. C. Cranfield, in *The Geology of Queensland*, P. A. Jell, Ed. (Geological Survey of Queensland, 2013), pp. 13–34.
20. G. Rosenbaum, The Tasmanides: Phanerozoic tectonic evolution of eastern Australia. *Annu. Rev. Earth Planet. Sci.* **46**, 291–325 (2018).
21. R. A. Henderson, C. L. Fergusson, I. W. Withnall, Coeval basin formation, plutonism and metamorphism in the Northern Tasmanides: Extensional Cambro-Ordovician tectonism of the Charters Towers Province. *Aust. J. Earth Sci.* **67**, 663–680 (2020).
22. R. A. Henderson, B. M. Innes, C. L. Fergusson, A. J. Crawford, I. W. Withnall, Collisional accretion of a Late Ordovician oceanic island arc, northern Tasman Orogenic Zone, Australia. *Aust. J. Earth Sci.* **58**, 1–19 (2011).
23. R. A. Henderson, C. L. Fergusson, Growth and provenance of a Paleozoic subduction complex in the Broken River Province, Mossman Orogen: Evidence from detrital zircon ages. *Aust. J. Earth Sci.* **66**, 607–624 (2019).
24. H. N. Dirks, I. V. Sanislav, A. S. A. A. Abu Sharib, Continuous convergence along the paleo-Pacific margin of Australia during the Early Paleozoic: Insights from the Running River Metamorphics, NE Queensland. *Lithos* **398–399**, 106343 (2021).
25. S. Tumiati, S. Martin, G. Godard, Hydrothermal origin of manganese in the high-pressure ophiolite metasediments of Praborna ore deposit (Aosta Valley, Western Alps). *Eur. J. Mineral.* **22**, 577–594 (2010).
26. H. P. Schertl, N. V. Sobolev, The Kokchetav Massif, Kazakhstan: "Type locality" of diamond-bearing UHP metamorphic rocks. *J. Asian Earth Sci.* **63**, 5–38 (2013).
27. X. Wang, J. G. Liou, H. K. Mao, Coesite-bearing eclogite from the Dabie Mountains in central China. *Geology* **17**, 1085–1088 (1989).
28. Y. C. Liu, X. F. Gu, F. Rolfo, Z. Y. Chen, Ultrahigh-pressure metamorphism and multistage exhumation of eclogite of the Luotian dome, North Dabie Complex Zone (central China): Evidence from mineral inclusions and decompression textures. *J. Asian Earth Sci.* **42**, 607–617 (2011).
29. H. P. Schertl, P. J. O'Brien, Continental crust at mantle depths: Key minerals and microstructures. *Elements* **9**, 261–266 (2013).
30. C. Chopin, Coesite and pure pyrope in high-grade blueschists of the Western Alps: A first record and some consequences. *Contrib. Mineral. Petrol.* **86**, 107–118 (1984).
31. E. J. Krogh Ravna, M. P. Terry, Geothermobarometry of UHP and HP eclogites and schists – an evaluation of equilibria among garnet–clinopyroxene– kyanite–phengite–coesite/quartz. *J. Metam. Geol.* **22**, 579–592 (2004).
32. R. Y. Zhang, S. M. Zhai, Y. W. Fei, J. G. Liou, Titanium solubility in coexisting garnet and clinopyroxene at very high pressure: The significance of exsolved rutile in garnet. *Earth Planet. Sci. Lett.* **216**, 591–601 (2003).
33. S. Song, L. Zhang, Y. Niu, Ultra-deep origin of garnet peridotite from the North Qaidam ultrahigh-pressure belt, Northern Tibetan Plateau, NW China. *Am. Mineral.* **89**, 1330–1336 (2004).
34. M. D. Ruiz-Cruz, C. Sanz de Galdeano, Diamond and coesite in ultrahigh-pressure–ultrahigh-temperature granulites from Ceuta, Northern Rif, northwest Africa. *Mineral. Mag.* **76**, 683–705 (2012).

35. D. S. Keller, J. J. Ague, Crystallographic and textural evidence for precipitation of rutile, ilmenite, corundum, and apatite lamellae from garnet. *Am. Mineral.* **104**, 980–995 (2019).
36. P. J. O'Brien, J. Rötzler, High-pressure granulites: Formation, recovery of peak conditions and implications for tectonics. *J. Metam. Geol.* **21**, 3–20 (2003).
37. L. Guo, H. F. Zhang, N. Harris, F. B. Pan, W. C. Xu, Late Cretaceous (~81Ma) high-temperature metamorphism in the southeastern Lhasa terrane: Implication for the Neo-Tethys ocean ridge subduction. *Tectonophysics* **608**, 112–126 (2013).
38. T. A. Alifirova, L. N. Pokhilenko, A. V. Korsakov, Apatite, SiO_2, rutile and orthopyroxene precipitates in minerals of eclogite xenoliths from Yakutian kimberlites, Russia. *Lithos* **226**, 31–49 (2015).
39. S. Haggerty, V. Sautter, Ultradeep (greater than 300 kilometers), ultramafic upper mantle xenoliths. *Science* **248**, 993–996 (1990).
40. H. S. Tomkins, R. Powell, D. J. Ellis, The pressure dependence of the zirconium-in-rutile thermometer. *J. Metam. Geol.* **25**, 703–713 (2007).
41. M. J. Kohn, A refined zirconium-in-rutile thermometer. *Am. Mineral.* **105**, 963–971 (2020).
42. M. J. Holdaway, Application of new experimental and garnet Margules data to the garnet-biotite geothermometer. *Am. Mineral.* **85**, 881–892 (2000).
43. C.-M. Wu, Original calibration of a garnet geobarometer in metapelite. *Minerals* **9**, 540 (2019).
44. R. Jedlicka, S. W. Faryad, C. Hauzenberger, Prograde metamorphic history of UHP granulites from the Moldanubian Zone (Bohemian Massif) revealed by major element and Y + REE zoning in garnets. *J. Petrol.* **56**, 2069–2088 (2015).
45. R. Tamblyn, M. Hand, D. Kelsey, R. Anczkiewicz, D. Och, Subduction and accumulation of lawsonite eclogite and garnet blueschist in eastern Australia. *J. Metam. Geol.* **38**, 157–182 (2020).
46. A. K. Bidgood, A. J. Parsons, G. E. Lloyd, D. J. Waters, R. M. Goddard, EBSD-based criteria for coesite-quartz transformation. *J. Metam. Geol.* **39**, 165–180 (2021).
47. J. E. Greenfield, R. J. Musgrave, M. C. Bruce, P. J. Gilmore, K. J. Mills, The Mount Wright Arc: A Cambrian subduction system developed on the continental margin of East Gondwana, Koonenberry Belt, eastern Australia. *Gondw. Res.* **19**, 650–669 (2011).
48. R. A. Glen, Refining accretionary orogen models for the Tasmanides of eastern Australia. *Aust. J. Earth Sci.* **60**, 315–370 (2013).
49. L. Moresi, P. G. Betts, M. S. Miller, R. A. Cayley, Dynamics of continental accretion. *Nature* **508**, 245–248 (2014).
50. G. Phillips, R. Offler, D. Rubatto, D. Phillips, High-pressure metamorphism in the southern New England Orogen: Implications for long-lived accretionary orogenesis in eastern Australia. *Tectonics* **34**, 1979–2010 (2015).
51. J. C. Aitchison, S. Buckman, Accordion vs. quantum tectonics: Insights into continental growth processes from the Paleozoic of eastern Gondwana. *Gondw. Res.* **22**, 674–680 (2012).
52. W. G. Ernst, J. G. Liou, Overview of UHP metamorphism and tectonics in well-studied collisional orogens. *Int. Geol. Rev.* **41**, 477–493 (1999).
53. Y. F. Zheng, L. Zhang, W. C. McClelland, S. Cuthbert, Processes in continental collision zones: Preface. *Lithos* **136-139**, 1–9 (2012).
54. M. Frezzotti, J. Selverstone, Z. Sharp, R. Compagnoni, Carbonate dissolution during subduction revealed by diamond-bearing rocks from the Alps. *Nat. Geosci.* **4**, 703–706 (2011).
55. S. C. Penniston-Dorland, M. J. Kohn, M. E. Manning, The global range of subduction zone thermal structures from exhumed blueschists and eclogites: Rocks are hotter than models. *Earth Planet. Sci. Lett.* **428**, 243–254 (2015).
56. M. Brown, T. Johnson, Metamorphism and the evolution of subduction on Earth. *Am. Mineral.* **104**, 1065–1082 (2019).
57. A. F. Holt, L. H. Royden, T. W. Becker, The dynamics of double slab subduction. *Geophys. J. Int.* **209**, 250–265 (2017).

Acknowledgments: We thank K. Blake from the Advanced Analytical Centre at James Cook University (JCU) for technical support during EPMA data collection and processing. A.E. would like to acknowledge and thank JCU for the Australian Government Research Training Program (RTP) Domestic Stipend Scholarship and the Economic Geology Research Centre (EGRU) at JCU for housing this research. We would like to thank M. Hand for discussions and suggestions. This manuscript was improved by the constructive reviews provided by M. Brown, J. Hermann, and an anonymous reviewer. **Funding:** We would like to thank the Geological Survey of Queensland for project funding. **Author contributions:** Conceptualization: A.E., I.V.S., and C.S. Methodology: A.E. and I.V.S. Investigation: A.E. and I.V.S. Visualization: A.E., I.V.S., and C.S. Supervision: A.E. and I.V.S. Writing—original draft: A.E. Writing—review and editing: A.E., I.V.S., P.H.G.M.D., and C.S. **Competing interests:** The authors declare that they have no competing financial interests. **Data and materials availability:** All data needed to evaluate the conclusions in the paper are present in the paper and/or the Supplementary Materials.

Submitted 24 January 2022
Accepted 24 May 2022
Published 8 July 2022
10.1126/sciadv.abo2811